EVALUATION OF ALKALI-AGGREGATE REACTION EXPANSION ON PEDRA DAM BY MATHEMATICAL MODEL

Alberto J. C. T. Cavalcanti[1], Marco A C Juliani[2*], Gustavo Tristão[2], João F. A. Silveira[3]

[1]Companhia Hidro Elétrica do São Francisco – CHESF
Rua Delmiro Gouveia 333, RECIFE, Brasil, CEP 50761-901.

[2]Ieme Brasil Engenharia Consultiva Ltda
Rua MMDC, 499, SÃO PAULO, Brasil, CEP 05510-021.

[3]SBB Engenharia
Rua Miguel Petroni, 1265, SÃO CARLOS, Brasil, CEP 13561-002.

Abstract

Pedra Dam, located in de Contas River, was constructed between 1964 and 1968. The Dam is a 60 m high buttress type structure with a total length of 408 m, composed of 17 non-overflowing abutment blocks and 7 central spillway sections.

In 1991 the presence of alkali-aggregate reaction (AAR) was detected in the concrete structures by petrographic analysis and electronic microscopy. The concrete expansion has caused horizontal movement of contraction joints between blocks and cracks in several locations. The non-overflowing blocks, adjacent to the spillway sections have pushed to spillway gates piers, causing problems to the left end spillway gate operation.

This paper presents the results of a three-dimensional model of the dam and foundation, built in order to evaluate the behavior of concrete structures with loading induced by the AAR and study remedial measures. The obtained results of the dam behavior to current stage and prediction to next 10 years have indicated some alternatives to mitigate the effect of AAR such as cutting expansions slots between the blocks next to the spillway.

Keywords: Alkali-aggregate reaction, mathematical model, remedial measures, nonlinear analysis

1 INTRODUCTION

The Pedra Dam, located in De Contas River, at the place named Pedra da Santa, 18 km upstream the city of Jequié, in the state of Bahia – Brazil, is a buttress type dam, built between 1964 and 1968. The dam has a power station with a nominal 48 MW Power Francis turbine generating unit.

The dam is composed by 24 blocks (Figure 1) – eleven of which are of the non-overflowing type – with an approximate total 187 m length on the right side and six blocks adding up to a total 102m on the left. Both sectors are connected to each other by seven spillway blocks with a total length of 119 m, with seven 9,0 m-high and 12,50m-wide radial-type gates. Gate openings are separated by 2,25 m-wide double piers. The spillway capacity is 8,000 m^3/s with the reservoir at elevation 231.00 m.

Each buttress head is 17 m wide. Blocks 10 and 11 have a 3m-diameter steel penstock. Block 11 penstock works as a bottom spillway, whereas at block 10 is the hydroelectric power intake. Maximum dam height above foundation is around 60m (elevation 232.00 m). Maximum normal reservoir level is elevation 228, 00 m whilst exceptional maximum and minimum levels are elevations 231,00 m and 208,00 m, respectively.

Each element cross section has a top-bottom increasing wide buttress, i.e., 6,74m-wide at the top and 10,50m at the foundation. Spillway blocks have geometric characteristics that are similar to non-overflowing blocks up to the elevation 200,64 m. Above this level, the block is shaped like an overflowing sill (Figure 2).

Alkali-aggregate reaction has been causing concrete expansion, which has lead to difficulties in operating the spillway left end gate. Besides, the reaction has caused other anomalies such as "map" type cracks on the dam crest and at the top of spillway trunnion beams; compression of the contraction joints between blocks at upstream, leading to joint filling bitumen exudation (Figure 3); contraction joints opening downstream, which is particularly visible at the trunnion beams region and sub-vertical tensile cracks on the gallery walls at the spillway.

* Correspondence to: mjuliani@iemebrasil.com.br

In view of such anomalies, studies were performed for evaluating present stress and deformation state on dam structural elements by using a three-dimensional mathematical model. In addition to this, remedial measures have been studied in order to mitigate alkali-aggregate reaction effects, aiming to assure good operating conditions of the spillway gates for the next 10 years.

2 ALKALI-AGGREGATE REACTION IN STRUCTURE

After first alkali-aggregate reaction occurrence suspicions at Pedra Plant, petrographic analysis performed in 1991 has shown such reaction to be incipient and to happen locally, apparently concentrated nearby exposed concrete surfaces (at the top of the core) and along with more deformed and finer grain aggregates. One sample feature that has proved the low intensity of AAR, was confirmed by the absence of radial cracking in the aggregates.

Coarse aggregates used in concrete correspond to high metamorphic rate, resistant and apparently unaltered gneiss rocks. The predominant minerals are high temperature alkaline feldspar and plagioclase quartz, showing greenly grey colour, medium-coarse grains and a slightly more evident layering. Besides, garnet, biotite and opaque elements were observed in a lower proportion.

Samples contained crystals within a broad range of dimensions and evidence of recrystallization. Quartz was often stretched, according to rock foliation, suggesting, thus, an intense deformation. Alkaline feldspar was also quite deformed.

Complementary tests with an electronic microscope were also performed with the goal of characterizing alkali-aggregate reaction products. The characterized reaction, in 1991, was of the alkali-silicate type of whose development was considered slow, having as reactive components strained quartz and also high temperature alkaline feldspar which occur in some coarse aggregates undergoing intense deformation process.

3 MATHEMATICAL MODEL DESCRIPTION

With the aim of simulating structure concrete expansion as well as studying possible remedial measures, a dam three-dimensional mathematical model was developed, including the concrete structure and the foundation mass.

3.1 Model general conception

The dam mathematical three-dimensional model was developed with the finite element software ANSYS. The modelling was done using the International System of Units (SI) and the global coordinate system was oriented as flollows (Figure 4):

X Axis: horizontal, upstream oriented – downstream and positive in this direction;

Y Axis: horizontal, along dam longitudinal direction and positive from left to right;

Z Axis: horizontal, vertical and positive upwards.

The following finite elements were used:

SOLID 92 – for the concrete and rock mass elements, being composed by ten nodes, having each one three degrees of freedom, referred to translations about the local x, y and z axes. This element is suitable for irregular meshes (tetrahedral elements) since it has a quadratic interpolation functions;

TARGE 170 and CONTAC 174 – for simulating contraction joints between concrete blocks, fundamental for transferring longitudinal stresses due to AAR expansion. TARGE170 was used to represent the 3-D "target" surfaces for the associated contact elements, defined by CONTAC 174. The contact elements themselves overlay the solid elements describing the boundary of a deformable body and are potentially in contact with the target surface. Each contraction joints was represented by one flexible-flexible contact pair. The contact elements work only when it reaches the target elements, transferring compression stress.

The model aimed to simulate the effects of concrete expansion in the whole dam, mainly the spillway piers surroundings. The complete model was composed by 71223 nodes and 40753 elements (Figure 5 and Figure 6). For block meshing some factors such as proportion within element three dimensions and degree of refinement were taken into account in order to obtain satisfactory results, having in view future remedial measures. Concrete block and rock mass nodes at the interface were coupled in all three directions.

3.2 Material properties

Material elastic properties

Material elastic initial properties used in modelling are presented in Table 1.

Concrete expansion

The calibration of the mathematical model of the Pedra Dam demonstrated the need to simulate the anisotropy of the concrete [1], adopting differentiated expansion rates for the vertical and horizontal directions. In the calibration, the models that presented the best fit were those that regarded horizontal expansion rates around 40% of those in the vertical direction. At the first ages, concrete expansion rate (εc) due to AAR, was taken as increasing up to a maximum value that was then kept constant from 5 years on.

Under a confining stress state, concrete expansion was simulated, varying as showed in Figure 7 adapted of [2]. This figure shows a diagram representing the evolution of expansion rates versus confining stress, in which it can be noticed that, the greater the compression confining stress is, the smaller is the expansion rate due to AAR.

Concrete viscoelastic behavior

Alkali-aggregate reaction changes some concrete viscoelastic parameters, increasing both the creep and the stress relaxation and also reducing the elastic modulus along time. For the creep function , the equation adopted by the U.S. Bureau of Reclamation was used:

$$f(k,t-k) = \frac{1}{E(k)} + F(k) \cdot \ln(1+t-k) \qquad (1)$$

where:
k = concrete age at loading, in days;
t = time under loading, in days.

A 15% reduction of the initial elastic modulus (E_o) was admitted for the 17 years old concrete, leading thus to the curve shown in Figure 8. The creep coefficient F(k) was determined from creep test results for the concrete of Paulo Afonso I, II, and III Power Plants [3]. Besides, for the one year old concrete test value from similar concrete was adopted and the curve shown in Figure 8 was adjusted.

From the creep coefficient F(k) and 1/E(k) parameters, the relaxation curves were calculated, according to the methodology presented in SOUZA LIMA et al. (1979) [4]. Figure 9 represents the relaxation curve for a load applied after 20 years.

Load application and boundary conditions

The nodes of the five (5) rock mass external faces (Figure 5) were restrained in all three directions, simulating, this way, mass continuity. Load application was done in steps as follows [5]:
STEP 1 (1969) – loading due to concrete self weight, hydrostatic loading and concrete shrinkage (-10ºC) were considered, using initial elastic parameters. Concrete stress relaxation was also considered;
STEP 2 (1970) – based on results obtained in the first step the expansion rates were calculated. Finite element node coordinates, as well as concrete viscoelastic properties for this age were also updated and then the expansions were applied, leading to the new stresses and deformations. Concrete relaxation was also performed;
STEP N – step 2 procedures were repeated, year by year, until the year of 2006.

For hydrostatic loads, the maximum normal water level (elevation 228,00 m) was considered. These loads were applied in the form of pressure on upstream block faces. Loads acting on closed gates (situation that occurs most of the time) were converted into forces and applied on the trunnion beams.

4 MODEL RESULTS

Results considering concrete expansion were calculated for several spots in the mathematical model, along 38 years. Figure 10 illustrates dam deformation after 38 years of expansion, in which the closing of contraction joints between non-overflowing blocks can be observed, leading to force transmission to the spillway gate piers.

Concrete expansion, at the end of 38 years, has resulted in displacement in Y direction (flow transverse direction), at the piers in contact with non-overflowing blocks, of 16.0 mm and -8.7 mm, respectively at B12 and B18. In block B12 this piers displacement was higher than that one for block B18, due to the longer length of the right abutment blocks.

Table 2 presents the reduction of gate lateral clearances, taking the measure at the downstream piers top as a reference. It could be observed that the clearance reduction at blocks B18 and B12 are similar,

despite the short length of the left abutment. It also stands out that obtained values for blocks B13 to B17 are much smaller. Reduction gate lateral clearances were also obtained in 3 points along the spillway gate line, for the critical blocks B12 and B18 (
Table 3).

Final displacements at the dam crest in the Z (vertical) direction were around 80 mm (Figure 11), which indicates a vertical mean expansion rate of 38.50 με/year. Displacement increase in X direction (parallel to flow) was around 10 mm. It also stands out that in the first year displacements in the Z direction were of, approximately, -10 mm due to self weight and shrinkage loadings and of 8 mm in the X direction (parallel to flow), due to hydrostatic loading.

Expansion has caused opening of the contraction joints at the trunnion beams region of 5.23 mm and 6.59 mm, between blocks B11 and B12 and blocks B18 and B19 respectively. Table 4 presents the opening and the sliding in the upstream-downstream direction, where no significant values could be noticed for the spillway interior blocks. Joints opening and sliding match the actual dam behaviour

The mathematical model was calibrated in a qualitative way, based on contraction joints movement, since there are no data from monitoring. According to performed inspections, all joints between non-overflowing blocks are closed at upstream region, as it can be observed from bitumen exudation. Joints between spillway blocks and between blocks B10-B11 and B18-B19 are open at both upstream and downstream regions, down to approximately elevation 220 m and closed below this elevation. Contraction joints behaviour was reproduced by the mathematical model after 38 years of expansion, as presented on Figure 12, pointing out that the gray colour indicates the open regions.

5 REMEDIAL MEASURES

Remedial measures studied for Pedra Dam had spillway gates clearance reduction as the main focus. This problem has caused difficulties in the operation of the left end gate and may shortly occur at the right end. As occurred at Mactaquac [6, 7], Hiwassee [8, 9] and Chambon [10, 11] dams, spillway side expansion slot cutting represents a feasible solution for attenuating the effects due to concrete slow expansion, caused by AAR.

At first, 10 slot cutting alternatives on the spillway both sides' blocks were evaluated, with different locations and cutting depths, as showed in table 5.

The slot cutting step was simulated in the mathematical model by means of applying the stress calculated, after 38 years of expansion, on the opposite direction in the elements along the slot plane. In additional, at the slot area, the contact element has been deactivated. In order to evaluate the remedial measures alternatives, a model with 48 years of expansion, without any remedial measures, has been taken as reference.

The slot cutting effectiveness evaluation can be done by comparing the reduction of the gate lateral clearances, at the point 1 along the gate line, in the critical blocks B12 and B18 (adjacent to non-overflowing blocks), as illustrated in
Table 3, against the slot cutting alternatives, as shown in Figure 13. According to the results, it could be observed that alternatives VI, VII, VIII and IX are more effective considering B12 and B18 gate clearances reduction. Besides, slot cuttings have provided longitudinal stress relief in the joints between blocks. This way, alternative IX has shown itself as a very effective one concerning joints 10 (B11-B12) and 17 (B18-B19) stress reduction along their heights (Figure 14).

6 CONCLUSIONS

Presented results have shown a high increase in displacements and stresses, after 38 years of expansion, compared to displacements and stresses due to self weight, hydrostatic and concrete shrinkage loading. As a result, actual anomalies in Pedra Dam can be explained by the occurrence of AAR.

The shown three-dimensional mathematical model, which simulated the effects caused by concrete expansion due to AAR, has shown results, stress and displacements, compatible to current stage Pedra Dam concrete structural elements properties.

The slot cutting alternatives that include the joints between the spillway and the adjacent non-overflowing blocks (joints 10 and 17) are more effective in decreasing the expansion thrust on the spillway piers. On the other hand, the alternatives with slot cutting on joints between non-overflowing blocks are less efficient but decrease the progression of expansion thrust on the spillway piers and have a cut area only 25% of the other alternatives.

Further studies by means of a more elaborated mathematical model are in progress in order to evaluate the feasibility of the remedial measures.

7 REFERENCES

[1] LARIVE, C. (1998): Apports Combines de Léxperimentation et de la Modélisation à la Comprehension de L'Alkali-Réaction et de ses Effects Mécaniques, LCPC, France.

[2] The Institution of Structural Engineers (1992): Structural Effects of Alkali-Silica Reaction. Technical guidance on the appraisal of existing structures, Chapter 5.

[3] SILVA P. N., CAVALCANTI, A. J. C. T., SANTOS, S. B, LOPES, A. N. M., HASPARYK, N. P. (2008). Creep of Concrete Cores Affected by the Alkali-Aggregate Reaction. 13th International Conference on Alkali-Aggregate Reaction, Trondheim, Norway.

[4] SOUZA LIMA, V. M; GUEDES, Q. M; ANDRADE, W. P. E BASTOS, J. T. (1979): Cálculo da Relaxação de Tensões a Partir da Fluência do Concreto. Revista Construção Pesada. Rio de Janeiro, Brasil.

[5] CAVALCANTI, A. J. T., JULIANI, M.A., IGUTI, E. T., HAHNER, I., ZUNIGA, J. E. (2004): AAR Effects at the Paulo Afonso IV Power Intake. 12th International Conference on Alkali-Aggregate Reaction, Beijing, China.

[6] THOMPSON, G.A., STEELE, R.R. (1992): Alkali Aggregate Reaction at Mactaquac Generating Station Remedial Measures Progress Report. I International Conference on Concrete Alkali-Aggregate Reactions in Hydroelectric and Dams, Fredericton, Canada.

[7] TOMPSON, G.A., STEELE, R.R., COULSON, D.M. (1995): Management of Concrete Growth at the Mactaquac Generating Station. II International Conference on Concrete Alkali-Aggregate Reactions in Hydroelectric and Dams, Chattanooga, USA.

[8] TANNER, D.T. (1992): The Use of Monitoring and Finite Element Analysis in Evaluating Remedial Measures at TVA`s Hiwassee Dam.

[9] NEWELL, V.; WAGNER, C. (1995): Modifications to Hiwassee Dam and Planned Modification to Fontana and Chichamauga Dams by the Tennessee Valley Authority to Manage Alkali-Aggregate Reaction.

[10] BEAUCHAMPS, T., GOGUEL, B. (1992): Gonflement et Projet de Confortement du Barrage du Chambon. I International Conference on Alkali-Aggregate Reactions in Hydroelectric Plants and Dams, Fredericton, Canada.

[11] BEAUCHAMP, T. (1995): The Progress of Remedial Measures at Chambon Dam. II International Conference on Concrete Alkali-Aggregate Reactions in Hydroelectric and Dams, Chattanooga, USA.

Table 1: Initial Elastic Properties.

Parameters	Concrete	Rock mass			
		Left shoulder	Right shoulder	Part 1	Part 2
Elastic modulus (MPa)	24000	14000	16000	20000	10000
Poisson's Ratio	0.2	0.2	0.2	0.2	0.2
Central part 1 – Mass below B10, B11, B12, B13, B17, and B18 (blue color at Figure 5). Central part 2 – Mass below B14, B15, and B16 (magenta color at Figure 5) .					

Table 2: Gate lateral clearances reduction (top of piers at downstream) of spillway blocks.

Clearance reduction (mm)	B12	B13	B14	B15	B16	B17	B18
	19.56	2.88	2.87	2.57	1.70	0.45	20.38

Table 3: Reduction of gate lateral clearances at spillway gate line (mm).

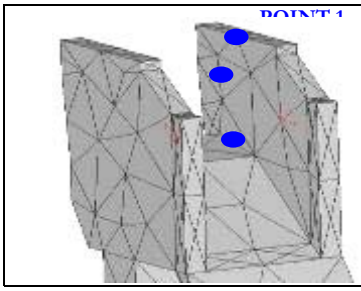

Points	Block 12	Block 18
1	17.18	17.29
2	9.03	10.03
3	1.79	1.63

Table 4: Joint behavior at the trunnion beams region.

Contraction Joint	Opening (mm) – Direction Y	Sliding (upstream-downstream) mm – Direction X
10 (B11-B12)	5.23	2.13
11 (B12-B13)	2.33	0.34
12 (B13-B14)	2.19	0.10
13 (B14-B15)	2.13	0.23
14 (B15-B16)	2.07	0.35
15 (B16-B17)	2.04	0.49
16 (B17-B18)	2.21	0.05
17 (B18-B19)	6.59	0.64

Table 5: Expansion slot cutting alternatives.

Alternative	Contraction joints /depth (m)							
	Right abutment				Left abutment			
	7 (B8/9)	8 (B9/10)	9 (B10/11)	10 (B11/12)	17 (B18/19)	18 (B19/20)	19 (B20/21)	20 (B21/22)
I				24	24			
II			20			20		
III			10.50			10.50		
IV		20					20	
V	20						20	
VI				16	16			
VII	20			16	16		20	
VIII			20	16	16	20		
IX			10.50	16	16	10.50		
X	20	20	20			20	20	20

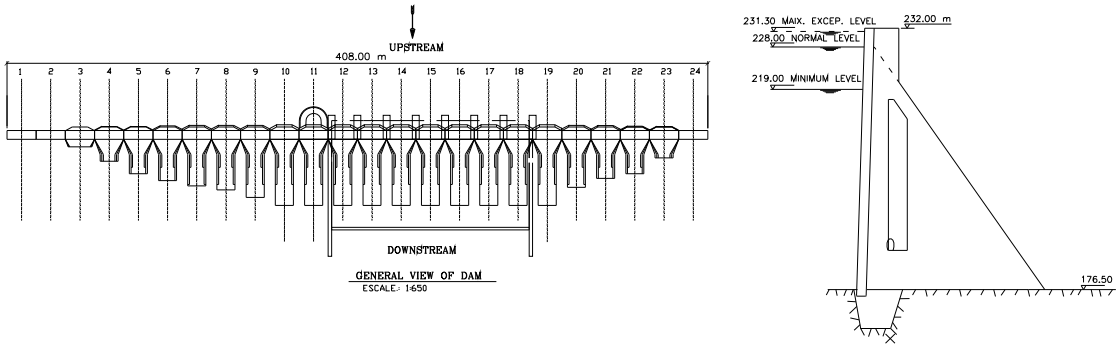

(a) (b)

Figure 1: (a) General view of Pedra Dam and (b) Cross-section of block 19.

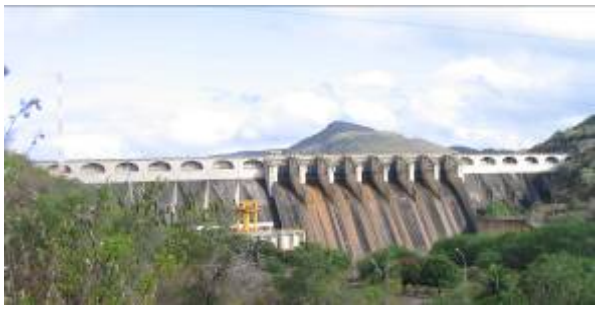

Figure 2: General downstream view of Pedra Dam.

(a) (b)

Figure 3: (a) Contraction joint with bitumen exudation (block B10-B11) and (b) Contraction joint between spillway piers at downstream with average 1 cm opening.

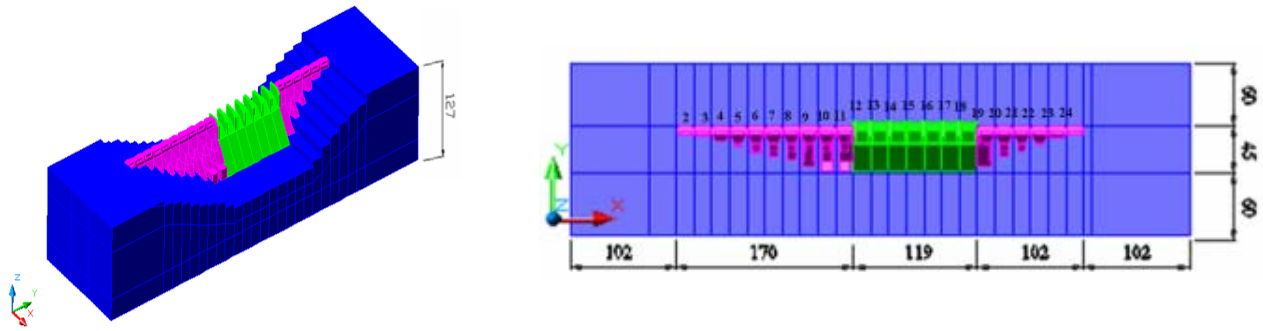

(a) (b)

Figure 4: (a) Three-dimensional view of model geometry (Dam and rock mass) and (b) plan view (block numbers) – dimensions in meters.

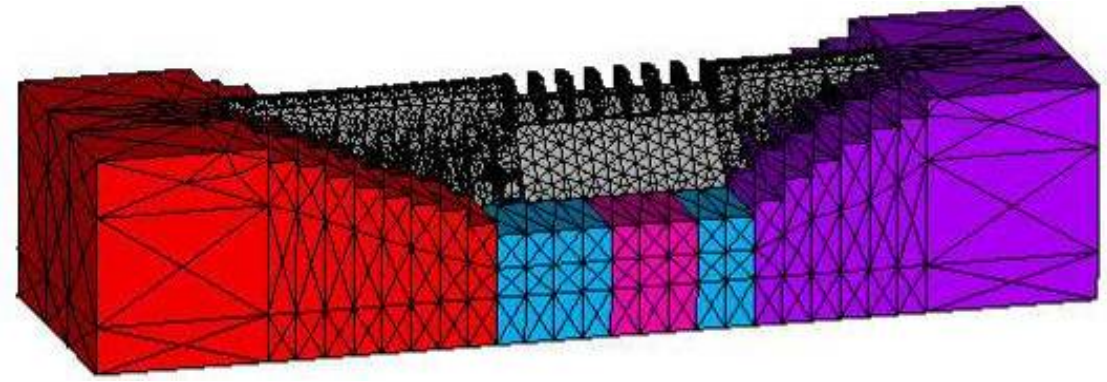

Figure 5: Whole model finite element mesh – perspective from downstream.

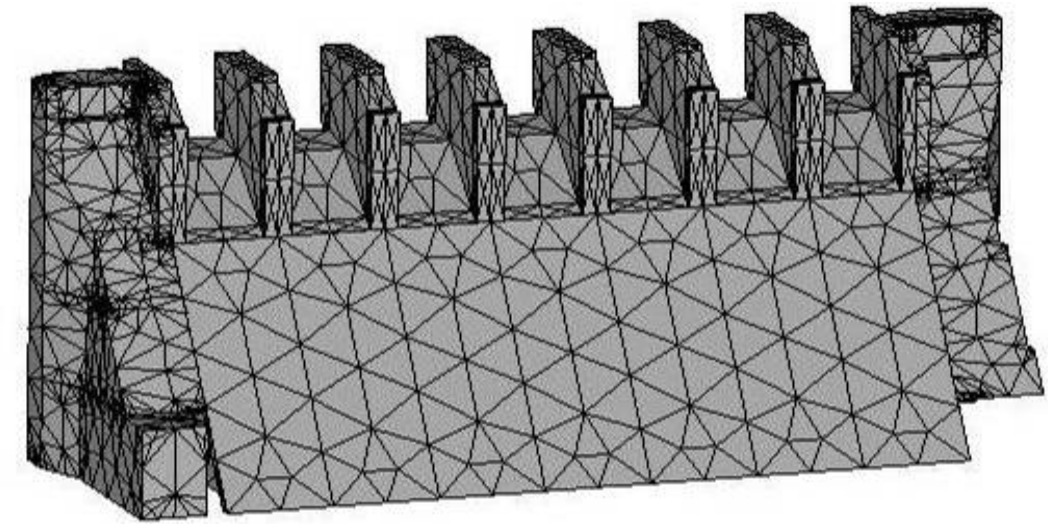

Figure 6: Spillway and B11 and B19 adjacent blocks finite element mesh.

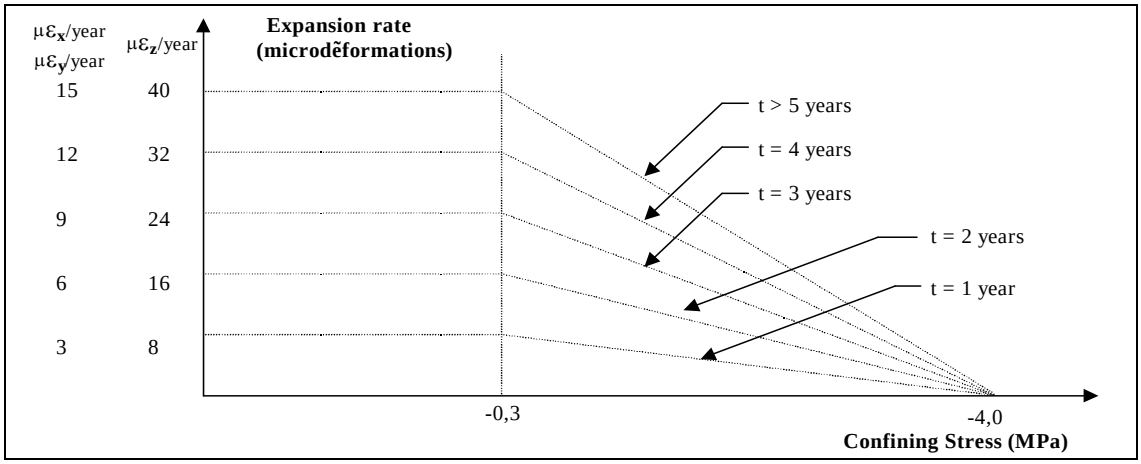

Figure 7: Expansion rates x confining stress (logarithmic scale).

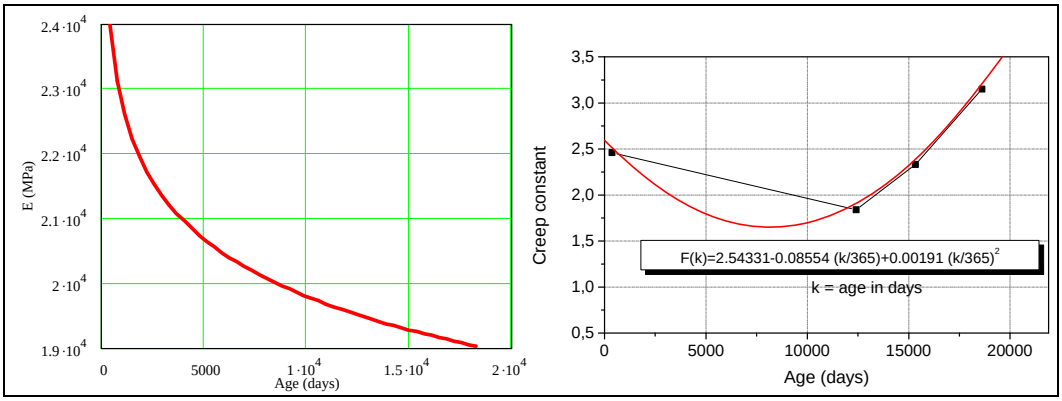

Figure 8: Elastic modulus E(k) and Creep coefficient F(k) curves.

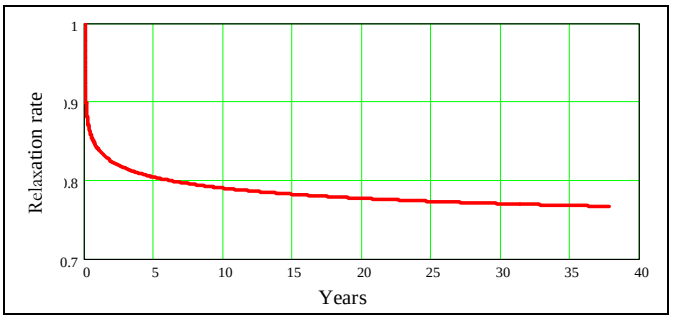

Figure 9: Relaxation curve for load applied after 20 years.

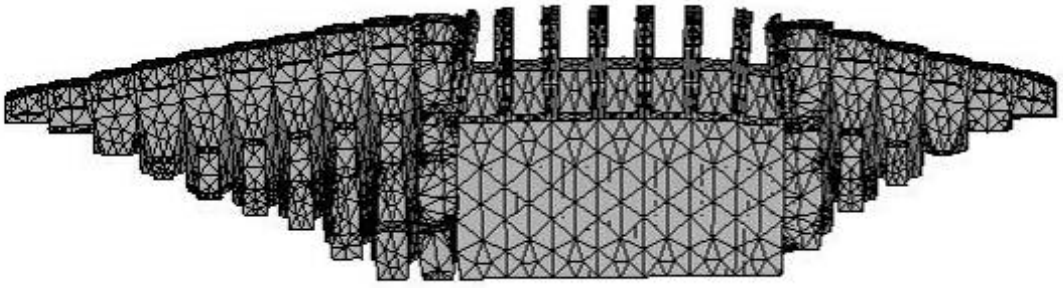
Figure 10: Dam deformation after 38 years of expansion – Downstream View.

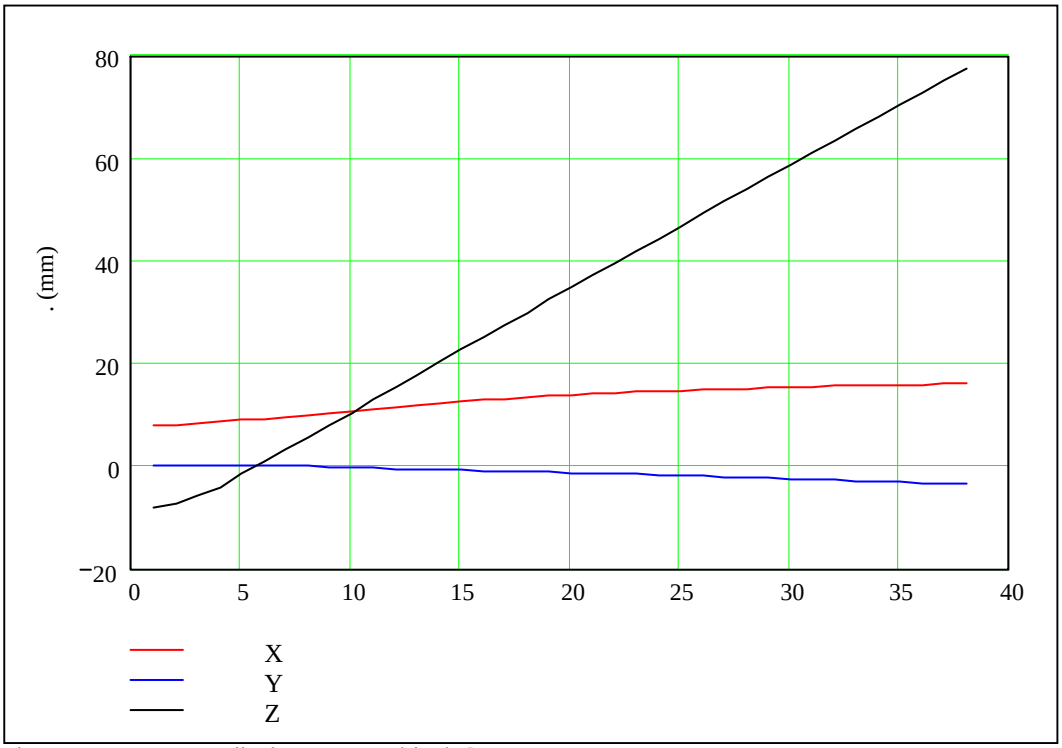

Figure 11: Dam crest displacements – block B12.

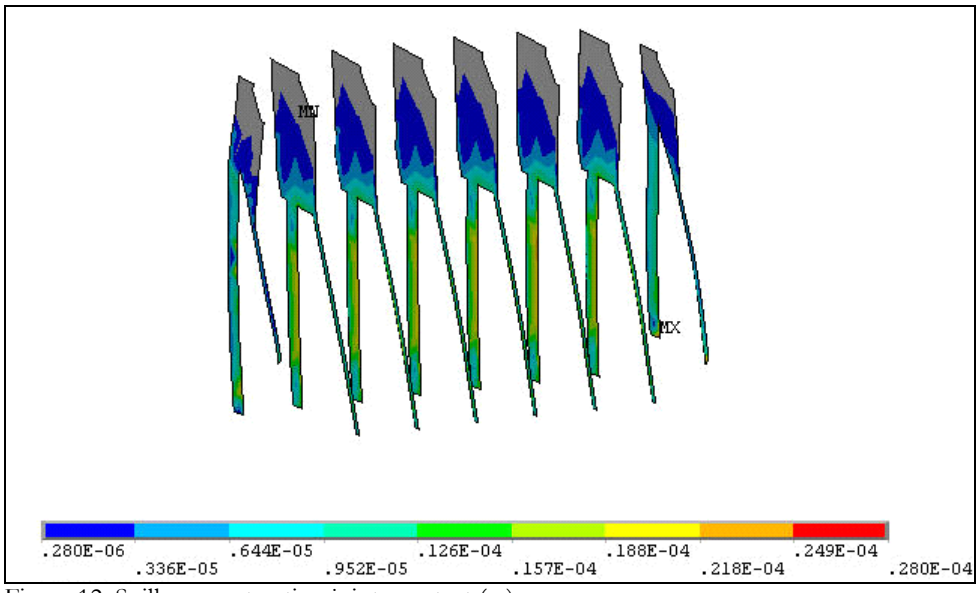

Figure 12: Spillway contraction joints contact (m).

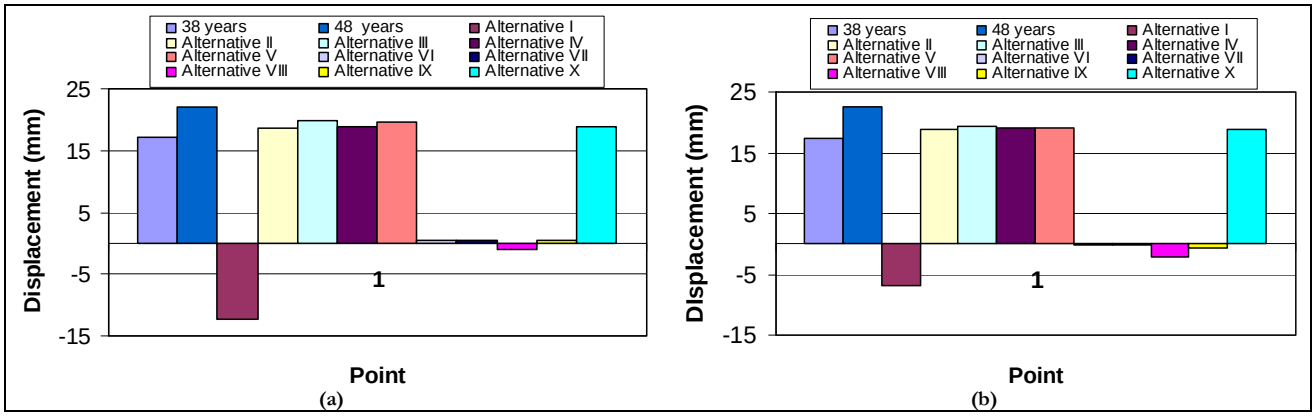

Figure 13: Reduction of spillway gate clearances (a) block 12 and (b) block 18.

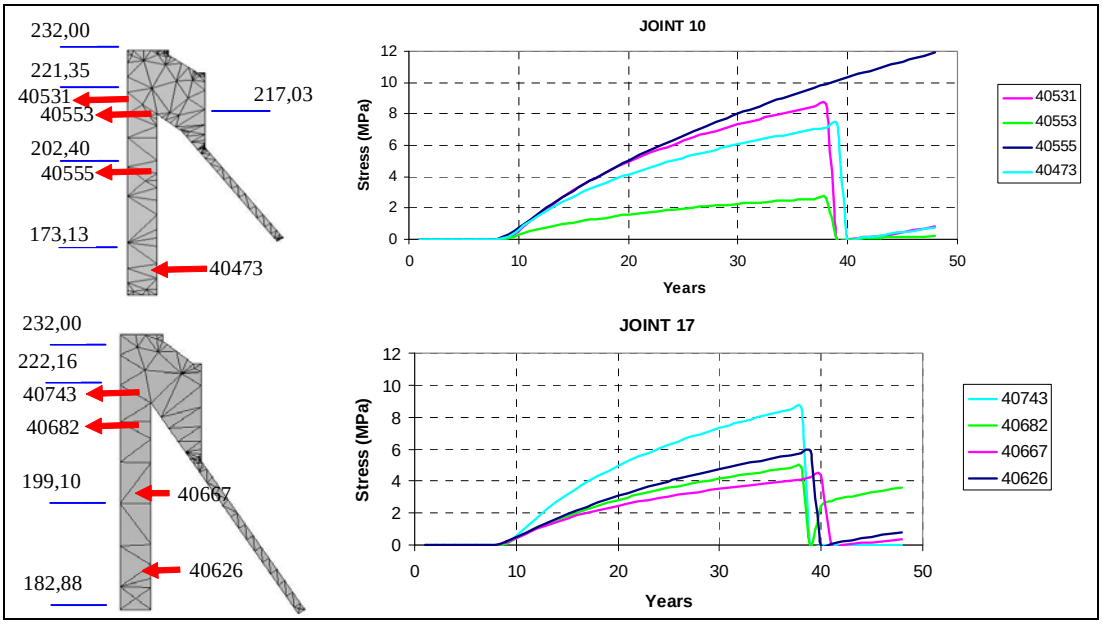

Figure 14: Longitudinal stress relief due to slot cutting – Alternative IX.